archives
of thermodynamics
Vol. **43**(2022), No. 1, 3–19
DOI: 10.24425/ather.2022.140922

Location-optimized aerodynamic rotor design studies and development of small wind turbines

DANIEL LEHSER-PFEFFERMANN
ALEXANDER HAMMAN
FRANK ULRICH RÜCKERT*

University of Applied Sciences Saarbrücken (htw saar),
Faculty of Economic Sciences, Campus Rotenbühl, Waldhausweg 14,
66123 Saarbrücken, Germany

Abstract Local wind conditions can vary strongly depending on the landmark and vegetation, as well as on the skyline of the buildings in an urban surrounding. Weather, season and time of day influence the yield of electric power. In order to promote the use of small wind turbines as an alternative to photovoltaic power generation, design optimization for location-optimized small wind turbines was carried out. In this work, we want to concentrate on vertical axis wind turbines. Experimental studies, as well as numerical simulations, have been conducted. On the one hand, bionically optimized core structures will be integrated and implemented in the hybrid material of the turbine blades. Several optimization attempts have been examined for single blades. Detailed simulative investigations with large eddy simulations improve the aerodynamic behaviour of the new rotor design. Finally, based on the results of the studies and investigations, a new rotor will be manufactured and tested experimentally in the wind tunnel. A comparison with the reference system from the first part of the paper shows the improvements and effectiveness of the measures and processes investigated.

Keywords: Small wind turbine; Fluid energy machines; Vertical axis wind turbine, Additive manufacturing, Fibre-reinforced composites; Computational fluid dynamics; Large eddy simulation; Turbulence simulation

*Corresponding Author. Email: frank.rueckert@htwsaar.de

Nomenclature

AOA	–	angle of attack
CFD	–	computational fluid dynamics
LES	–	large eddy simulation
WALE	–	wall-adapting local eddy-viscosity
VAWT	–	vertical axis wind turbine

1 Introduction

The field of fluid energy machines is one of the most sophisticated topics in engineering. In this work, the rotor design process is described and investigated. For this purpose, the boundary conditions were first determined by wind measurements for the local conditions at the htw saar campus (*Hochschule für Technik und Wirtschaft des Saarlandes* University of Applied Sciences) have been conducted [1]. Based on these data, a rotor parameter study was performed and a combination of Darrieus H- and O-rotor was defined. An additive manufacturing process was used for the production of the rotor, which ensured the necessary mechanical properties with a hybrid material approach. With improved mechanical properties, it was possible to reduce the amount of material required. Finally, the adapted and designed prototype was measured in the wind tunnel. In this part of the work, further adjustments and optimizations will now be carried out based on the results already obtained.

The aerodynamic profile of the turbine blades was considered and adjusted. With the use of additive manufacturing, further optimization approaches arise by making better use of the possibilities of this manufacturing process. A more detailed investigation of the flow pattern within the rotor and in the wake that forms concludes the optimization process. Finally, the improved rotor is compared with the reference system from the first part of the paper.

In order to keep the losses within the rotor low, turbulence development at the whole turbine and stall effects at the blades should be reduced to a minimum. For this purpose, various parameter studies were carried out on the basis of the system developed. The rotor design itself was finally defined, so in this part of the work, the adaptation of the linkages as well as the rotor drive train itself can be investigated.

1.1 Turbine design and electric generator

The position of the generator is discussed first. In the reference design, this is arranged centrally in the middle of the rotor. This arrangement leads to the formation of a Karman vortex street in the centre of the rotor. Studies of Rezaeiha *et al.* show that there is a correlation between the diameter of the axles and the losses that occur [2]. This finding, applied to the current rotor, leads to two possible alternative positions of the generator. One possibility would be to position it at the top of the rotor. This would place the generator outside the rotor and reduce vortex development inside the rotor. However, there are also some disadvantages. The cable from the generator to the inverter must pass through the axis, which is why a hollow axis is necessary. In addition, assembly and maintenance are significantly more complex in this position.

A better option here is positioning at the lower end of the rotor as shown in Fig. 1. The generator and the connection are located outside the rotor, are more easily accessible and thus easier to reach during installation and maintenance. Such positioning is also advantageous from the point of

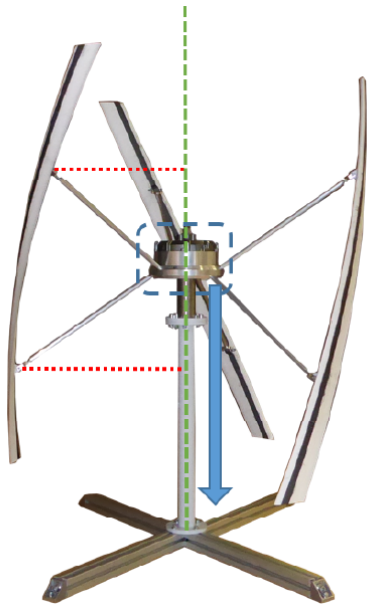

Figure 1: Modifications to the vertical axis wind turbines (VAWT) drive train and to the rotor to reduce turbulence-induced losses.

view of plant dynamics, as the centre of gravity of the plant is shifted downwards towards the foundation. This reduces the extreme loads and fatigue loads that occur. These conclusions can also be derived from the simulation results and confirm them.

1.2 Connection of the blades

In a further study, the positioning and design of the connection of the blades were investigated [1]. With the repositioning of the generator, the connection must also be changed. To reduce the strut length, the first approach is to replace the V-shaped connection with a horizontal connection. The degree of rotational freedom on the blade is retained. This allows a reduction of the loads at the connection. However, the connections within the rotor still result in losses due to additional vortex developments. For another variant, the connection is moved to the ends of the blades. This reduces the vortex development inside the rotor caused by the connection to a minimum. There are also aerodynamic advantages to this variant. Due to the further development of the profile with a smooth transition to the connection, blade tip losses can be reduced. The new connection acts like a winglet at the blade tip.

Combined with the hybrid material insert, it is also possible to reduce the loads at the connection. The previously used rotational degree of freedom is converted into a spring element. This spring function can be easily integrated after design, dimensioning and manufactured without any additional effort. This allows the rotor blade to twist in itself and thus compensate for stresses within the blade. The drive torque is then mainly transmitted at the connection and transferred from the blade to the generator axis through the fibre composites.

1.3 Structure and airfoil geometry

The weight of the single blades is crucial for the yield. Based on structural analysis of tensions with a commercial finite element solver Ansys Mechanical [3] and taking into account the manufacturing process, the core structure of the rotor blades can be further improved. Through bionically inspired structures and their implementation in the core, the material can be chosen according to requirements. Inside the profile, a bionically inspired core structure is integrated by additive manufacturing. The core structure is adapted accordingly based on the structure simulation as described by [4].

The geometry of the structure was designed by a numerical algorithm and is influenced by the tensions inside the blade geometry and weight optimisation. The algorithm to generate the inner structure was used with commercial Rhino 6 and Grashopper [5]. Grasshopper is a visual programming tool to create rules and parameters that can be easily changed and updated, tightly integrated with Rhino's 3D modeling tools.

All details about the wind turbine as well as tip speed ratio were described in detail in [6]. The blades are bent and have a length of 1.20 m. The nominal speed is about 6 m/s. With the use of hybrid material, the necessary mechanical properties can be achieved through the fibre composite material.

Figure 2 shows the integration of the core structure in the rigid part of the profile, i.e. in the leading edge area. This structure was printed with polyactide (PLA) and additional carbon fibre. Overall, the material consumption can be reduced by 30% compared to the reference of a solid structure. The mechanical properties in terms of deflection and strength were even slightly improved. Grashopper was also used to generate the stereolithography file for 3D printing. The core structure is arranged in such a way that, in the event of increased mechanical demands, the structure is also reinforced accordingly, this is shown by an increase in the cross-sections.

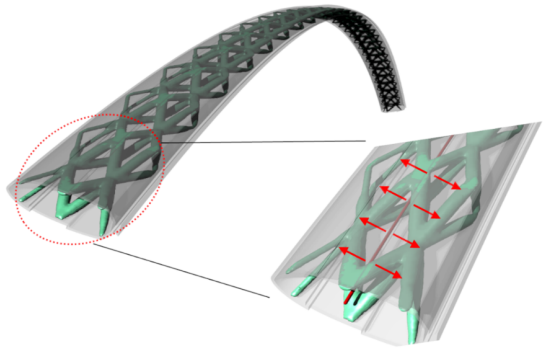

Figure 2: Bionically inspired core structure in the leading edge of the rotor blade.

2 Blade design and optimization

Optimization of the full vertical axis wind turbine (VAWT) can also be achieved with high performance blades. For basic blade design, the in-house developed software tool VAWT_power was used. It was developed and de-

scribed in detail in Lehser–Pfeffermann *et al.* [7]. To study and optimize the airfoil profiles, experiments in our small-scale Eiffele-type wind tunnel have been conducted [6]. Parameter studies performed with the VAWT_Power tool were based on the NACA0018, NACA0021 and NACA0012 data sets. To optimize the base profiles further, different optimization approaches were investigated and their influence on the aerodynamic coefficients was discussed.

2.1 Optimization approaches for blade design

Using the boundary conditions from the measurements of further work [1], Reynolds numbers (Re) on the blade profile are obtained for the later operating range. A comparison of the lift and drag coefficients was carried out with an interactive program for the design and analysis of subsonic isolated airfoils – XFoil [8]. A total of 30 different profiles are examined in the parameter study. As a result of this study, as it is described in [6], it is shown that DU 06-W-200 profile is best suited for the local boundary conditions considered. Based on this design, more sophisticated optimization strategies have been examined. But only two of the approaches investigated will be described here in detail. Once an optimum profile has been found, the two approaches to aerodynamic influence can be integrated. These approaches are in detail a flexible trailing edge as well as vortex generators. The other is the flexible trailing edge as described and studied by Beyene *et al.* [9–11].

Since the purpose of this work was to develop a robust system with the lowest possible maintenance requirements, we tried the so-called "vortex generators" based on the work of Kerho *et al.* in theWheeler ramped cone structure [12]. It is already known that on the shroud side of a turbine blade, the so-called "Görtler" swirls can produce high risks of stall [13,14]. Chaotic fluctuating turbulence swirls will lead to lower forces and efficiencies. To minimize this influence of the Görtler swirls, small cones can be positioned on the top side of the airfoil. The concept is shown in Fig. 3.

With the help of the vortex generators, a targeted transition from the laminar to the turbulent boundary layer is achieved. The turbulent boundary layer that develops stabilizes the flow and thus leads to a later detachment of the boundary layer. The reason for this is the formation of ordered vortices, which reduce a flow transversely along the blade. In addition, the transition area from laminar to turbulent flow is reduced. These effects reduce the losses due to turbulence on the airfoil and thus also ensure an increase in the stall angle and a reduction in drag. A Wheeler structure

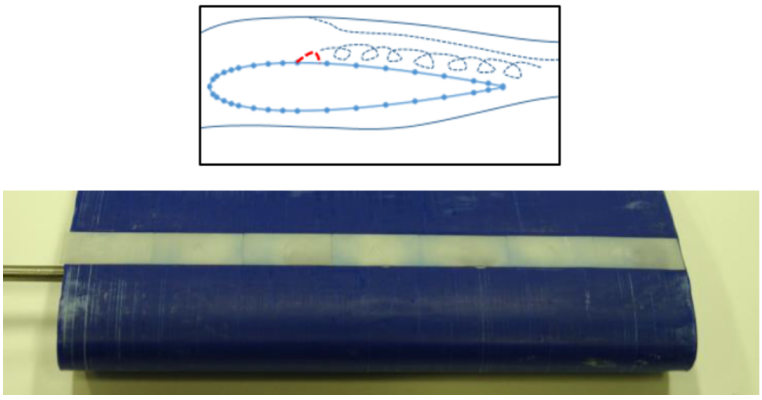

Figure 3: Turbine blade design with vortex cone to prevent Görtler swirls and stall effects.

with a structure height of 80% of the local boundary layer proves to be promising [12]. The arrangement of the airfoils at the height of the aerodynamic centre relative to the chord length defines the position at the top half of the airfoil.

For the flexible trailing edge shown in Fig. 4, a compromise must be found in terms of stiffness/flexibility with regard to the subsequent operating range. The trailing edge is to be designed flexibly to adapt to the changed flow at higher angles of attack (AOA), especially in the stall angle range. This allows the flow to detach from the geometry later and higher lift coefficients can be achieved. At the same time, the profile must not be too flexible to avoid unacceptable deformation due to Coriolis forces. For this

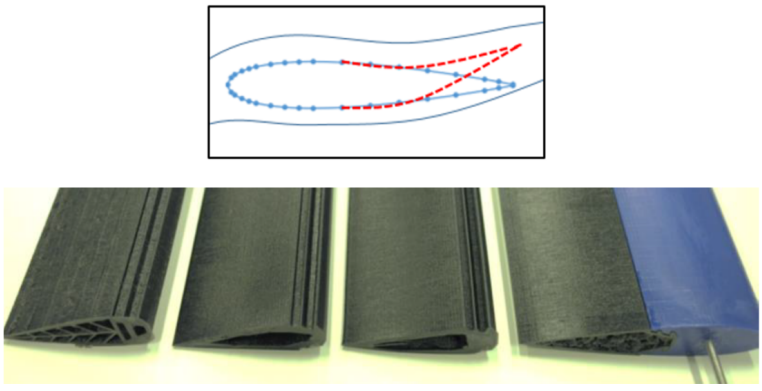

Figure 4: Turbine blade design with flexible trailing and different inner structures.

purpose, the subsequent speed operating range must be defined in order to perform a corresponding estimation. A corresponding study was conducted in [7]. This results in a filling ratio of around 5% for the core structure with a constant wall thickness of approximately 0.001 m. The trailing edges have been 3D printed with a flexible elastomer.

2.2 Experimental investigations of single blades

Experimental investigations of the optimized airfoil profiles described before are shown in Figs. 5 to 7. The experiments were carried out in a wind tunnel with Eiffler design in our laboratory, which has been described in detail in [6]. The nozzle size in the tunnel is 0.25 m × 0.25 m and maximum air velocities of 25 m/s are possible. The airfoils can be rotated to change the angle of attack according to the fluid stream and forces are measured on two axes with pressure sensors. Fluid velocities have been measured with an anemometer. The lift and drag curves are plotted against the angle of attack. Values refer to a Reynolds number of Re = 80 000, which represents the average operating range between Re = 40 000 and 140 000. We have examined different air velocities but we will concentrate on Reynolds numbers Re = 80 000 here.

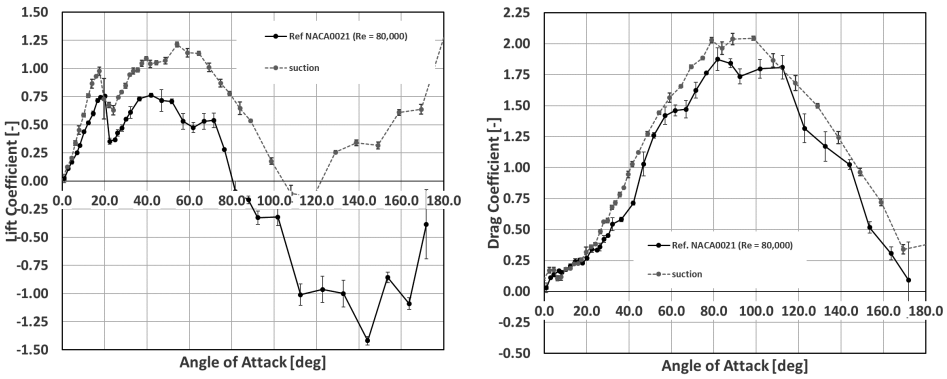

Figure 5: Experimental results from the optimized airfoil for aerodynamic coefficients at Re = 80 000.

Based on the XFoil simulation, different optimization steps for the airfoil build the base for our development. In Fig. 5 it can be seen that this first optimization step will lead to approximately 20% higher lift forces. The meaning of the different ploted lines will be explained.

The left side of Fig. 5 shows the lift coefficient versus the angle of attack. The reference profile (NACA0021) is shown as characteristic dark line. A column shows the deviation. It is possible to shift the stall angle to higher angles of attack (AOA) with the abovementioned optimisation. In addition, a higher lift coefficient before stall is achieved with the optimized profile. For higher AOA, the adjusted profile with suction shown with the grey doted line is shifted parallel. On the right side, the drag coefficient is shown over AOA. The reference profile is again shown as line in dark. The optimized profile corresponds to the course of the reference profile taking into account the measurement inaccuracy and the standard deviation. For the other Reynolds numbers investigated, the optimized profile is below the reference profile in grey dotted lines. This shows the effects of the optimization with regard to the reduced drag. The blades have been rotated in the tunnel to realize different AOA. At an AOA of about 12°, it can be clearly seen that the stall effect occurs. This will lead to lower lift forces and a huge decrease in the efficiency of the whole wind turbine. Even geometry modifications cannot prevent the occurrence of stall. The drag coefficient is not influenced by stall.

Different designs of the cones were tested. Moreover, it can be said that they will lead to different drag coefficients, depending on their structure. In Fig. 6 the results of an investigation with the vortex generator are shown. In addition, stall effects will be shifted to higher AOA, which will result in a more efficient wind turbine. The results for the flexible trailing edge can be seen in Fig. 7. Flexible edges lead to higher lift coefficients as well as to a decrease in drag, which will increase the overall efficiency of the turbine.

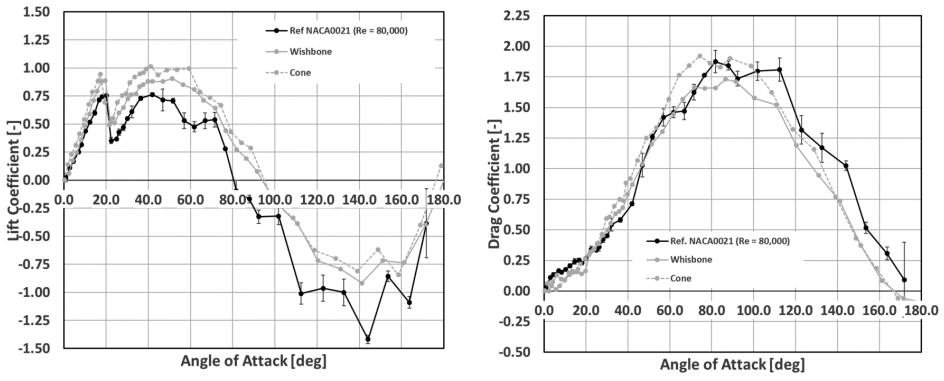

Figure 6: Experimental results from airfoil with swirl generator for aerodynamic coefficients at Re = 80 000.

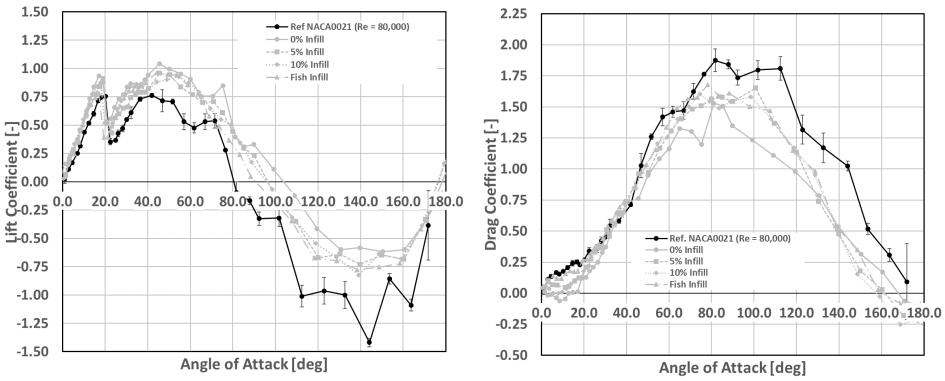

Figure 7: Experimental results from airfoil with flexible tail for aerodynamic coefficients at Re = 80 000.

3 Numerical simulation of full-scale turbine

After the aerodynamic profiles are adjusted and a lightweight adaptation of the blades is implemented, the entire rotor can be further investigated with a full turbine model. The possibilities of prototype production from hybrid material allow further adjustments. Additionally, to examinations in our large wind tunnel Göttingen-type [1, 7] and numerical simulations of the fluid flow have been done with the commercial computational fluid dynamics (CFD) program for turbomachinery applications – Ansys CFX [3]. The simulation was also done for a wind tunnel with Göttinger design [6] and a nozzle width of 1.6 m × 1.6 m. Maximum fluid velocities in the large-scale wind tunnel are 9.0 m/s.

3.1 Turbulence description

The overall optimization of the blades together with the full turbine can only be done by a numerical full-scale model. At least we want to introduce a quantity to evaluate it. To be able to estimate the efficiency of the turbine, we examine the production of turbulence and swirl around the geometry of the overall turbine [15]. A good quantity to judge the efficiency, is the turbulent viscosity, μ_t. Strong turbulence generation is always inefficient. The turbulent viscosity and laminar viscosity, μ_l, result in an overall total viscosity:

$$\mu_{\text{total}} = \mu_l + \mu_t \,. \tag{1}$$

It can be said that higher quantities of viscosity will lead to higher shear and losses. The turbulent viscosity or eddy viscosity is based on the turbulent kinetic energy, k, and the rate of dissipation of turbulence, ϵ:

$$\mu_t = \rho C_\mu \frac{k^2}{\epsilon}\,, \tag{2}$$

where ρ is the density of air and C_μ is a constant (normaly it is approx. 0.09). It has been used in the present paper where the additional stresses arise out of turbulent fluctuations in the momentum equations. The turbulent or eddy viscosity is defined by the following relationship:

$$\mu_t = \frac{\left(S_{ij}^d S_{ij}^d\right)^{\frac{3}{2}}}{\left(\overline{S_{ij}}\,\overline{S_{ij}}\right)^{\frac{5}{2}} + \left(S_{ij}^d S_{ij}^d\right)^{\frac{5}{4}}}, \tag{3}$$

where S_{ij}^d is the two dimensional stress tensor inside fluid in different coordinate directions $(i, j = 1, 2)$, and $\overline{S_{ij}}$ is the mean value of the stress tensor in every direction $(l, j = 1, 2)$, in this formula over bar denotes and symbol represents mean values.

The field distribution of the turbulence kinetic energy k and its dissipation rate ϵ, which is a measure of turbulence length scale, is obtained from the solution of the relevant transport equations. These equations for the turbulence scalars are not strictly valid in the viscosity dominated near-wall region of the wind tunnel.

3.2 Discretisation and force model

For discretisation of the surrounding of the wind turbine commercial Ansys ICEM CFD software package, which provides advanced geometry/mesh generation [16, 17], and block-structured hexahedral meshes were used to prove the high quality of the numerical results. With the three-dimensional (3D) flow simulations, a better understanding of the turbulence development within the rotor and in the direct wake of the turbine can be examined [15]. To model the rotating turbine, the block-structured meshes have to be designed with two different domains.

The simulation domain is shown in Fig. 8. One rotating domain with the turbine inside and a static surrounding fluid of the tunnel, which is not moving. To couple the two meshes we used general grind interfaces (GGI),

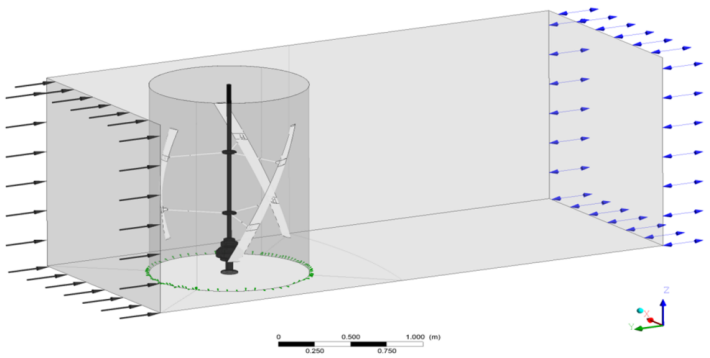

Figure 8: Simulation of the static and rotating domain of the wind turbine inside the Göttingen-type tunnel.

feature from CFX. In addition, a standard approach for the wall function is used in the present algorithm for the near-wall cells.

To rotate the mesh that directly surrounds the wind turbine, we have to calculate the forces at the blade and calculate the momentum. This is directly coupled with the numerical simulation, which means that the rotational speed of the moving domain is a direct result of the absolute inflow velocity. A sketch of the model and the force calculation is shown in Fig. 9. So not only the production of turbulence is a result of numerical

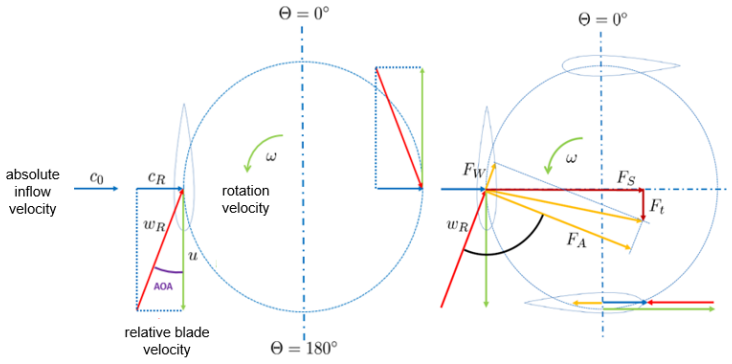

Figure 9: Force model for the calculation of the rotation velocity of the turbine mesh: c_0 – absolute inflow velocity, c_R – velocity on the blade, w_R – resulting velocity, u – circumferential velocity, AOA – angle of attack, ω – rotational velocity, Θ – degree of rotation of the turbine, F_S – forces on the blade, F_t – offset force, F_W – resulting force on blade, F_A – acting force on blade.

simulation but also the rotation of the domain itself. This explains why simulation of a full-scale turbine can only be done in conjunction with rotational meshes.

3.3 Numerical results and validation

The investigations are first carried out with different turbulence models as described by Ahmed *et al.* [16–18]. As a result, detailed investigations should be carried out using large-eddy approaches. Turbulence fluctuations and fluid forces on the blades induce the forces. A simple force model was used to induce the rotation velocities for the rotating domain. An interim result of this parameter study is shown in Fig. 10. The artificially introduced eddy viscosity is shown, which is calculated with the help of the wall adapting local eddy viscosity model, which is designed for large-eddy simulation (LES-WALE) [3, 18, 19]. The eddy viscosity shows the forming eddies and can be interpreted and analyzed accordingly.

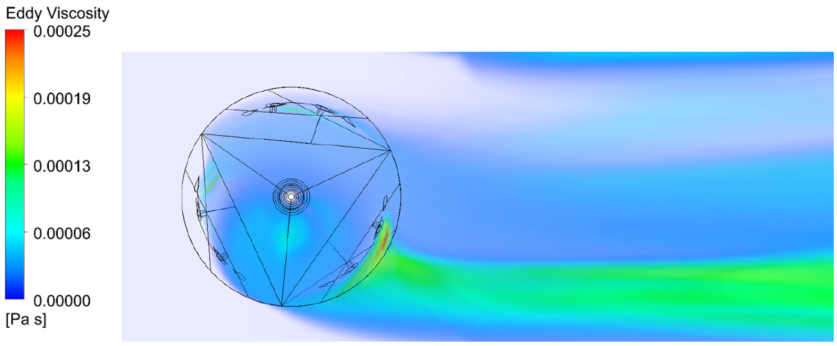

Figure 10: Simulation of the flow wake of the VAWT see from the top at wind velocity 10.0 m/s.

Investigations of the wake show that the velocity distribution is not symmetrical. Due to the rotation of the rotor, the corresponding flow velocities overlap. If the flow distribution is viewed from above the rotor, as shown in Figure 10, this effect becomes apparent. In the area where the rotor moves with the flow, the effect is small. In the opposite case, the flow is strongly decelerated after the turbine. The already mentioned asymmetric wake is formed with a vortex concentration in the area of the opposite flow directions. This effect has a high influence on efficiency and must therefore be taken into account when positioning subsequent installations.

In Fig. 11 we present a visualisation of an isosurface of the eddy viscosity. This is caused by the vortices that are formed due to the stall and movement of the rotor blades. At the bottom of the rotor, blade tip losses and the boundary of the rotor are also clearly visible.

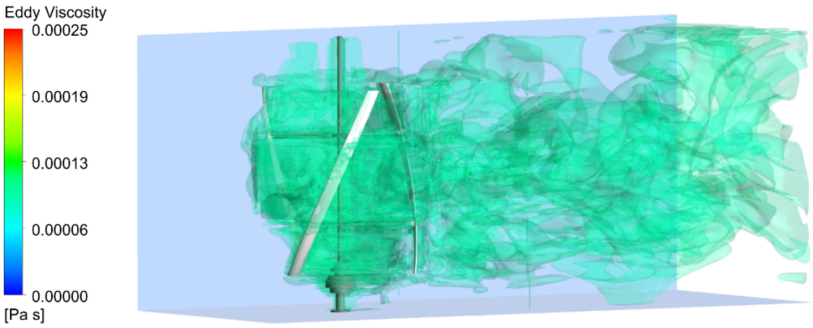

Figure 11: Isosurfaces of the eddy viscosity at VAWT and the wake region at wind velocity10.0 m/s.

In addition, the lower position of the electric generator can be seen. An increase in speed in the lower wall area can be explained with the help of the reference measurement in the duct without a test specimen. Isosurfaces give an idea where regions of similar eddy viscosity could be observed. The figure gives an impression of the quality of the model. Less sophisticated turbulence models only give mean values. Here we can directly evaluate the fluctuations. This means that also stall effects could be predicted. Therefore, LES is mandatory for such examinations but will lead to very high simulation times and costs.

To validate the CFD model, measurements in the aerodynamic test rig can be used. For this purpose, the modelled rotor is manufactured as a prototype and measured in the wind tunnel. Figure 12 shows a corresponding result compared to the simulation result. The measurements were done with an automatized Prandtl test tube on a raster of half of the wind tunnel. For this purpose, the entire measurement section is traversed in a 0.1 m $\times$ 0.1 m grid. On the right side in Fig. 12, the measured wind speed in the flow plane is shown as a contour plot. At each measuring point, 25 measured values were recorded and the arithmetic mean is calculated, which provides the basis for the velocity distribution. The plot on the left side of Fig. 12 shows the mean values of the measurements, as described in detail in [4]. By calculating the mean values, the unsteady behaviour of the VAWT wake can be characterised. By analising the areas of equal velocity ranges, the influence

of the rotor can be detected. On the right side of the figure a cut through the simulation, results presented also in Fig. 11 is visualised, which gives an impression of the wake structure. In the upper area of the measuring section, the blade tip losses can be easily recognized as decreasing wind speed. These show the developing vortex. In the central area of the rotor, a strong gradient to the central axis can be seen.

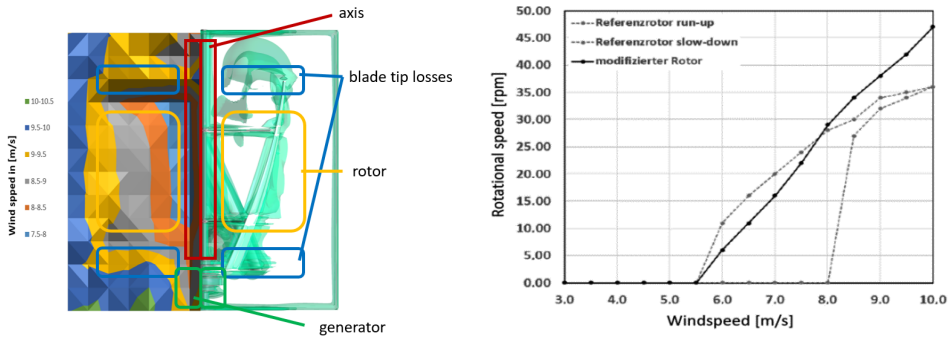

Figure 12: Comparison of the wind tunnel flow fields with large-eddy simulation (left) and measured turbine speeds as the result of experimental investigations (right).

In the right part of the figure, the results of the LES calculations are shown as eddy viscosity. In direct comparison with the experimental measurements, the same areas can be clearly defined and assigned. Large eddies resulting from rotor boundary and blade tip losses are well visible in the upper part of the figure. The vortex thereby turns in the direction of the rotor axis and thus forms the largest influencing factor on the wake flow in the upper edge area of the rotor. The rotation in the direction of the centre can also be well explained by the reference measurements without the test specimen and the resulting flow conditions due to the wall flow.

Additional experimental investigations of different turbine designs in the large scale wind tunnel show that the modified rotor can improve the system behaviour. The cut-in speed is reduced by 25%. At the same time, the maximum examined speed increases by 30% [1].

4 Conclusions

In a direct comparison between the reference wind turbine and the modified design, the following can be stated after completion of the various parameter studies. With the use of the hybrid material and the additive

manufacturing technology, the rotor weight can be reduced by 30% in total. This increases the mechanical load capacity and reduces deformation under load. By skilful selection of the core structure, these properties can be well adapted and implemented according to the requirements. The airfoil is selected and aerodynamically modified according to the subsequent Reynolds range. A flexible trailing edge and the use of vortex generators increase the lift coefficients and shift the stall effect to higher angles of attack. At the same time, the drag coefficient can be reduced, which also results in a positive effect on the system behaviour.

With this comparison, the effectiveness of the investigated measures and optimization approaches can also be proven experimentally. In addition, the comparison with the simualtion models shows that they have a realistic turbine behaviour. It is therefore possible to work with validated simulation models for future work and to implement further investigations on the basis of the CFD analysis.

Received 4 August 2021

References

[1] Lehser-Pfeffermann D., Häfele T., Rückert F., Griebsch J., Müller T., Joos F.: *Location-optimized aerodynamic design of small wind turbines and lightweight implementation using additive hybrid material*. Mech. Mech. Eng. **22**(2018), 2437–445.

[2] Rezaeiha A., Kalkman I., Montazeri H., Blocken B.: *Effect of the shaft on the aerodynamic performance of urban vertical axis wind turbines*. Energ. Convers. Manage. **149**(2017), 616–630.

[3] https://www.ansys.com/ (accessed 4 April 2021).

[4] Lehser-Pfeffermann D., Häfele T., Lehmon D., Hamman A., Griebsch J., Rückert F.: *Aerodynamically and structurally optimized rotor of a vertical axis small wind turbine for suburban areas*. In: Proc. ICCE2019 – 8th Int. Conf. Exhib. on Clean Energy, 12-14 August, Montreal, Canada, 2019.

[5] https://www.rhino3d.com/de/6/new/grasshopper/ (accessed 5 April 2021).

[6] Lehser-Pfeffermann D.: *Untersuchung des Strömungsverlaufes einer Rotorkonzeptstudie für vertikale Kleinwindkraftanlagen*, PhD thesis, Helmut-Schmidt Univ., Hamburg 2021.

[7] Lehser-Pfeffermann D., Theis D., Hamman A., Rückert F.: *Investigation and evaluation of aerodynamic efficiency improvement measures for vertical axis small wind turbines*. In: Proc. 6th Int. Conf. on Renewable and Non-Renewable Energy, Miami, May 20–21, 2019.

[8] http://web.mit.edu/drela/Public/web/xfoil/ (accessed 15 March 2021).

[9] MacPhee D., Beyene A.: *Performance analysis of a small wind turbine equipped with flexible blades*. Renew. Energ. **132**(2019), 497–508,

[10] Hoogedoorn E., Jacobs G., Beyene A.: *Aero-elastic behavior of a flexible blade for wind turbine application: a 2d computational study*. Energy **35**(2010), 2, 778–785.

[11] MacPhee D., BeyeneA.: *Fluid-structure interaction of a morphing symmetrical wind turbine blade subjected to variable load*. Int. J. Energ. Res. **37**(2013), 1, 69–79.

[12] M. Kerho, S. Hutcherson, R.F. Blackwelder, R.H. Liebeck: *vortex generators used to control laminar separation bubbles*. Int. J. Aircraft **30**(1993), 3, 315–319.

[13] Koehler R.: *Wirbel und Schrauben in Scherströmungen*. Elemente der Naturwissenschaft **20**(1974), 8–25.

[14] Taneda S.: *Experimental investigation of the wakes behind cylinders and plates at low reynolds numbers*. J. Phys. Soc. Japan **11**(1956), 3, 302–307.

[15] Benim A.C., Epple B., Krohmer B.: *Modelling of pulverised coal combustion by a Eulerian-Eulerian two-phase flow formulation*, Prog. Comput. Fluid Dyn. **5**(2005), 6, 345–361.

[16] Ahmed A., Ibrar B., Lehser-Pfeffermann D., Theis D., Benim A., Rückert F., Joos F.: *Investigation of wake flow and turbulence development behind small wind turbines*. In: Proc. ICREN – 2019 Int. Conf. on Renewabl, Paris, 24–26 April, 2019.

[17] Staśko T., Majkut M., Dykas S., Smołka K.: *Selection of a numerical model to predict the flowin a fan with a cycloidal rotor*. Arch. Thermodyn. **42**(2021), 4, 3–15.

[18] Marchewka E., Sobczak K., Reorowicz P., Obidowski S.D., Jóźwik K.: *Application of overset mesh approach in the investigation of the Savonius wind turbines with rigid and deformable blades*. Arch. Thermodyn. **42**(2021), 4, 201–216.

[19] Lipian M., Dobrev I., Massouh F., Jozwik K.: *Small wind turbine augmentation: Numerical investigations of shrouded- and twin-rotor wind turbines*. Energy **201**(2020), 117588.